

# Solar energy storage in $\text{Cs}_2\text{AgBiBr}_6$ halide double perovskite photoelectrochemical cell

*Kiran Prabhu, Aravind Kumar Chandiran\**

Department of Chemical Engineering, Indian Institute of Technology Madras, Adyar, Chennai, Tamil Nadu, India – 600036.

## I. Materials:

Cesium bromide (CsBr, 99.9% metals basis), silver bromide (AgBr, 99.5% metals basis), bismuth bromide (BiBr<sub>3</sub>, 99% metals basis), cobalt (II) chloride (98%), and dimethyl sulfoxide (DMSO, 99.9% ACS grade) were purchased from Alfa Aesar. Methyl viologen dichloride hydrate (MV<sub>2</sub>Cl<sub>2</sub>.xH<sub>2</sub>O, 98%), ammonium hexafluorophosphate (NH<sub>4</sub>PF<sub>6</sub>, >95%), tetrabutylammonium hexafluorophosphate (TBAPF<sub>6</sub>, 98%), 2,2'-bipyridyl (reagent plus, >99%), nitrosyl tetrafluoroborate (NOBF<sub>4</sub>, 95%) were purchased from Sigma Aldrich. Lithium(trifluoromethanesulfonyl)imide (LiTFSI, 98% purity) was purchased from TCI, Japan. Carbinol (CH<sub>3</sub>OH, HPLC gradient grade), and acetonitrile (CH<sub>3</sub>CN, HPLC gradient grade) were purchased from Finar. Acetone (analytical grade), hydrochloric acid (HCl, ACS grade 37%) and diethyl ether (analytical grade) were purchased from Rankem. Titanium tetrachloride (TiCl<sub>4</sub>, 99.5% extrapure) was purchased from Loba Chemie. 1,1,2,2-Tetrachloroethane (C<sub>2</sub>H<sub>2</sub>Cl<sub>4</sub>, analytical grade >99%) was purchased from Spectrochem. Transparent conducting glass substrates (FTO, TEC7, 2.2mm thick) and TiO<sub>2</sub> paste (DSL 18NR-T) were purchased from Dyesol (Australia). DSV ion-exchange membrane was purchased from Selemion, Japan. All the materials except FTO and membrane were used as received without any further treatment.

## II. Methods:

### II.a. TiO<sub>2</sub> substrate preparation:

The FTO glass substrates were first cleaned by ultrasonication in isopropanol for 20 minutes, followed by acidified water (few drops of HCl added to water) for 20 minutes. The substrates were then ultrasonicated again in fresh isopropanol and sintered at 500°C to remove any organic residues. The cleaned FTO substrates were coated with two blocking layers of TiO<sub>2</sub> by chemical bath deposition, using a solution of 40mM TiCl<sub>4</sub>, in a hot air oven at 75°C for 30 minutes. The deposited films were sintered at 500°C. A mesoporous TiO<sub>2</sub> scaffold was prepared by screen printing the nanoparticle TiO<sub>2</sub> paste (DSL-18NRT) using a 90T mesh screen, and the printed device was sintered by using a stepwise ramp rate to reach 500°C and then cooled to room temperature. The mesoporous film was again coated with an overlayer of TiO<sub>2</sub> by chemical bath deposition using a 40mM TiCl<sub>4</sub> solution and finally sintered at 500°C before further processing.

### II.b. Perovskite synthesis:

Cs<sub>2</sub>AgBiBr<sub>6</sub> was synthesized using a solution processing technique, where BiBr<sub>3</sub>, AgBr, and CsBr in the ratio 1:1:2 was dissolved in DMSO, by continuous stirring and then sintered at 275°C for a phase transition.<sup>1</sup>

### II.c. MV<sub>2</sub>PF<sub>6</sub> preparation:

MV<sub>2</sub>PF<sub>6</sub> was prepared as per the procedure reported elsewhere in the literature.<sup>2</sup> 55mg (0.2mmol) of 1,1 dimethyl-4,4'-bipyridium dichloride and 65mg (0.4mmol) of ammonium hexafluorophosphate were dissolved in 10ml of DI water. The water bath was heated to 70°C with constant stirring to obtain a clear solution. The solution was immediately cooled by immersion in an ice bath for the crystals to form. The solution was centrifuged, and the mother liquor was discarded. The crystals were again dissolved in DI water at 70°C and then cooled for the recrystallization process. The crystals were dried in a vacuum oven at 80°C for 36 hours.

### II.d. Pre-treatment of DSV membrane:

The DSV ion-exchange membrane is a chloride ion conducting membrane. In order to impart PF<sub>6</sub><sup>-</sup> conductivity, a pre-treatment was done to replace the chloride ion by PF<sub>6</sub><sup>-</sup>. The membranes

were taken in a Schlenk flask and dried under vacuum to remove all the water present. A 2M solution of TBAPF<sub>6</sub> in acetonitrile was introduced into the container, and membranes were left to equilibrate for five days before further use.

#### **II.e. Cobalt mediator preparation:**

Cobalt mediator was prepared as per the procedure reported elsewhere in the literature.<sup>3</sup> 3.7g cobalt(II) chloride hexahydrate was dissolved in DI Water (18.2MΩ Millipore). 8.4g 2,2-bipyridine dissolved in methanol and was slowly added to the above solution dropwise while stirring at 50°C to obtain cobalt(II)tris(bipyridine)dichloride. 32.65g lithium bis(trifluoromethanesulfonyl)imide was dissolved in DI water and slowly added to the above solution dropwise while stirring to obtain cobalt(II)tris(bipyridine)(TFSI)<sub>2</sub> precipitate. Above precipitate was filtered and washed with DI water and cobalt(II)tris(bipyridine)(TFSI)<sub>2</sub> wet powder is dissolved in ethanol at 60°C and slowly cooled and left for two days in the refrigerator for recrystallization to get pure cobalt(II)tris(bipyridine)(TFSI)<sub>2</sub>.

7g of cobalt(II)tris(bipyridine)(TFSI)<sub>2</sub> was dissolved in acetonitrile, and nearly 5g of NOBF<sub>4</sub> was added to it to oxidize Co(II) to Co(III). To exchange the counterion from BF<sub>4</sub><sup>-</sup> to TFSI<sup>-</sup>, the obtained product was dissolved in a mixture of acetone and methanol, and 10.7g of LiTFSI dissolved in DI water was added to the solution. The remaining solvent was filtered, and the wet powder is dissolved in ethanol and slowly cooled in the refrigerator for recrystallization for 2 days. Ethanol was filtered, and Co(III) crystals obtained are kept for drying under vacuum at 60°C for 1 day.

#### **III. Characterization:**

Electrochemical charge and discharge experiments were carried out on a two-electrode configuration in a Biologic SP300 potentiostat. The photoelectrochemical measurements were carried out by using a LED array (visible light-emitting), which was driven using a Keysight E3643A power supply, and the light intensity was calibrated to 100 mW/cm<sup>2</sup> intensity using a Hamamatsu S1787-12 photodiode. The solar cell J-V characteristics were measured under a 150W Xe-arc lamp (ScienceTech Instruments) which is calibrated to AM 1.5G spectrum using a reference photodiode. The chopping studies were carried out using an in-house designed mechanical chopper built using an Arduino UNO microprocessor. The structural characterization of the perovskite film was done by X-ray diffraction (D8 Advance, Bruker) using Cu-Kα source. The elemental compositions were studied with the help of Energy Dispersive X-ray spectroscopy (Quanta 200 FEG). The absorption spectrum of the powder from the scrapped films was carried using a Shimadzu (UV 2600) spectrometer fitted with an integrating sphere. The FTIR spectrum of the electrolyte was acquired using an Agilent Cary (630 FTIR) spectrometer. The emission studies were carried out using Horiba spectrofluorimeter (Fluorolog-3). The self-discharge studies were carried out by custom-made setup by modifying the sample holder of the Fluorolog-3, to carry out the emission studies *insitu* during the charge and discharge cycles. A Keithley SMU 2450 was integrated along with Fluorolog-3 to carry out the charge-discharge measurements.

#### **IV. Solar cell assembly:**

The PEC solar cell with a geometric area of 6.25cm<sup>2</sup> and active area of 2.25cm<sup>2</sup> were fabricated by using a perovskite photoanode and a platinized FTO as a counter electrode, with two silicone gasket spacer of thickness 1.5mm each (uncompressed thickness), and the electrodes were held together by binder clips. The electrolyte was injected into the cell by using

Schlenk transfer protocol. Platinization was by drop-casting a 5mM  $\text{H}_2\text{PtCl}_6$  ethanol solution on clean FTO followed by heating to 400°C for 20 minutes.

#### IV.a. Optimization of parameters in solar cells:

- (i) **Solvent:** The effect of the solvent composition on the performance was analyzed. The  $\text{TiO}_2$  mesoporous scaffold was prepared by screen printing technique, and the perovskite film was spin coated with a preheated (75°C) precursor solution (268mg of  $\text{BiBr}_3$ , 112.8 mg of  $\text{AgBr}$  and 254mg of  $\text{CsBr}$  in 1.4ml of DMSO). After spin coating, the films were annealed for 2 hours at 75°C for better adhesion followed by high temperature annealing at 275°C for 5 minutes. The two sets of devices varied by the solvent composition of the electrolyte were made. One set had  $\text{Co}^{2+}/\text{Co}^{3+}$  (10mM in 10:1 ratio) with TCE and ACN (90% tetrachloroethane and 10% acetonitrile v/v) solvent while the other set had the same redox mediator composition but had TCE and ethanol (90% tetrachloroethane and 10% ethanol v/v). The stability of the devices was monitored under light soaking for 20 hours with periodic monitoring of J-V characteristics, and it was found that the devices having solvent TCE and ACN in 90:10 ratio performed better. Figures S4 and S5, show the open-circuit potential, short-circuit current density, and the images of the films taken before and after the stability test. One can notice that film with TCE/ethanol electrolyte is either degraded or dissolved.
- (ii)  **$\text{TiO}_2$  scaffold:** The effect of differing thickness and method of  $\text{TiO}_2$  scaffold preparation, namely one-time screen printing, two-times screen printing, one-time spin coating, and two-times spin coating on the performance was analyzed. The perovskite film was spin-coated from a preheated (75°C) precursor solution (268mg of  $\text{BiBr}_3$ , 112.8mg of  $\text{AgBr}$  and 254mg of  $\text{CsBr}$  dissolved in 2.25ml of DMSO). After spin coating, the films were annealed for 2 hours at 75°C for better adhesion followed by high temperature annealing at 275°C for 5 minutes. The PEC solar cells were filled with  $\text{Co}^{2+}/\text{Co}^{3+}$ (10mM in 10:1 ratio) in a (90% tetrachloroethane and 10% acetonitrile v/v) solvent. The J-V characteristics revealed that the devices having two-time screen printed  $\text{TiO}_2$  performed better (Figure S6).
- (iii) **Preheating temperature:** The effect of preheating temperature of the precursor solution and 1<sup>st</sup> annealing step on the performance as the temperature was varied from 60°C to 90°C was analyzed. A two-time  $\text{TiO}_2$  screen printed scaffold was used and the perovskite film was spin-coated from a preheated (at various temperatures) precursor solution (268mg of  $\text{BiBr}_3$ , 112.8mg of  $\text{AgBr}$  and 254mg of  $\text{CsBr}$  dissolved in 2.25ml of DMSO). After spin coating, the films were annealed for 2 hours at the same temperature as the preheating temperature, followed by high temperature annealing at 275°C for 5 minutes. The PEC solar cells were filled with  $\text{Co}^{2+}/\text{Co}^{3+}$ (10mM in 10:1 ratio) in a (90% tetrachloroethane and 10% acetonitrile) solvent. The J-V characteristics revealed that the devices with a preheating temperature of 75°C performed better (Figure S7).
- (iv) **Precursor DMSO dilution volume:** The effect of varying precursor concentration of on the film thickness on the performance was analyzed by using various solvent volumes of DMSO, i.e., 1.4ml to 3.5ml with a fixed amount of precursors (268mg of  $\text{BiBr}_3$ , 112.8mg of  $\text{AgBr}$  and 254mg of  $\text{CsBr}$ ). A two-time  $\text{TiO}_2$  screen printed scaffold was

used, and the perovskite film was spin-coated from a preheated (75°C) precursor solution dissolved in DMSO. After spin coating, the films were annealed for 2 hours at 75°C for better adhesion followed by high temperature annealing at 275°C for 5 minutes. The PEC solar cells were filled with  $\text{Co}^{2+}/\text{Co}^{3+}$  (10mM in 10:1 ratio) in a (90% tetrachloroethane and 10% acetonitrile) solvent. The J-V characteristics revealed that the devices with a precursor DMSO dilution volume of 2.25ml performed better (Figure S8).

## **V. Photoelectrochemical solar rechargeable battery:**

### **(i) Positive electrode (Compartment 1):**

A 6.25cm<sup>2</sup> FTO substrate was etched in the middle by using zinc dust and HCl. TiO<sub>2</sub> substrate was prepared on one half of the electrode using the same techniques as mentioned earlier, while the other half of the electrode was masked using a polyimide tape during the processing steps. The bottom half was platinized following the procedure given in the solar cell assembly section. A two-time TiO<sub>2</sub> screen printed scaffold was used, and the perovskite film was spin-coated from a 2.25 ml DMSO solution containing 268mg of BiBr<sub>3</sub>, 112.8mg of AgBr and 254mg of CsBr, preheated at 75°C. The spin-coated films are annealed for 2 hours at 75°C followed by 275°C for 5 minutes.

### **(ii) Negative electrode (Compartment 2):**

A 6.25cm<sup>2</sup> FTO substrate was etched in the middle by using zinc dust and HCl. Both the halves were platinized before use.

### **(iii) Electrolyte preparation:**

**(a) Positive electrolyte preparation:** 10mM of  $\text{Co(II)(bipyridine)}_3(\text{TFSI})_2$ , 1mM of  $\text{Co(III)(bipyridine)}_3(\text{TFSI})_3$ , 10mM of TBAPF<sub>6</sub> was dissolved in a solvent (80-90% tetrachloroethane and 10-20% acetonitrile) and it was ultrasonicated well before use.

**(b) Negative electrolyte preparation:** 10mM of  $\text{MV}_2(\text{PF}_6)_2$  and 10mM of TBAPF<sub>6</sub> was dissolved in acetonitrile.

Both the electrolytes were purged with nitrogen gas before use, and they were introduced into the device by utilizing the Schlenk line transfer protocol to maintain the air-free atmosphere inside the device.

### **(iv) Battery assembly:**

The cell was assembled by using the same silicone gasket with the pretreated DSV membrane as a separator, and the cell was held in place by binder clips. Gold-coated copper shims were used to make contact from the device. The photoanode and the platinized electrode facing it were used during charging, and the other halves were used during discharging with two other gold-coated copper strips.

The photoelectrochemical solar rechargeable batteries are charged at 100μA and discharged at 5μA. The charge-discharge curves are given in Figures 2(a), S11 and S12.

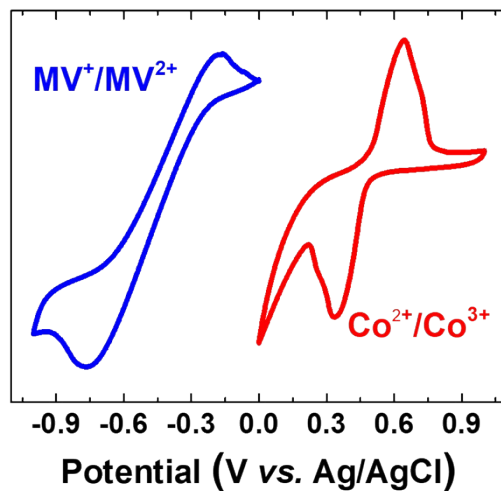


**Figure S1.** Cyclic voltammograms of  $Co^{2+}/Co^{3+}$  (in TCE/ACN 90/10 v/v mixture) and  $MV^+/MV^{2+}$  (in ACN) measured in a three-electrode system

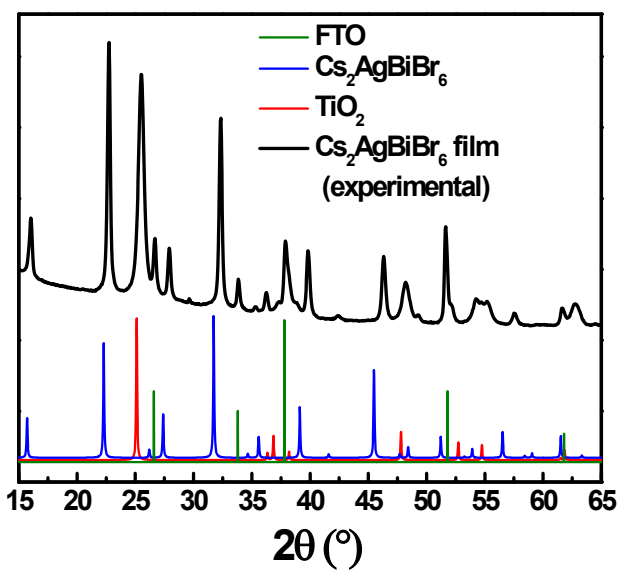


**Figure S2.** X-ray diffractogram of the photoelectrode used in the PEC device.

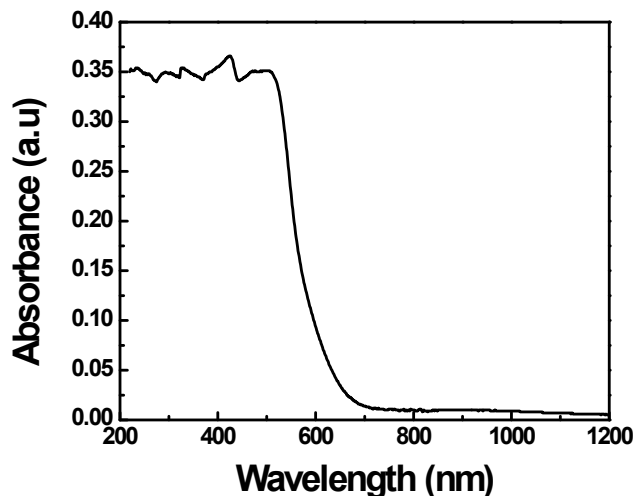


**Figure S3.** Optical absorbance spectra of the  $\text{Cs}_2\text{AgBiBr}_6$  photoelectrode.

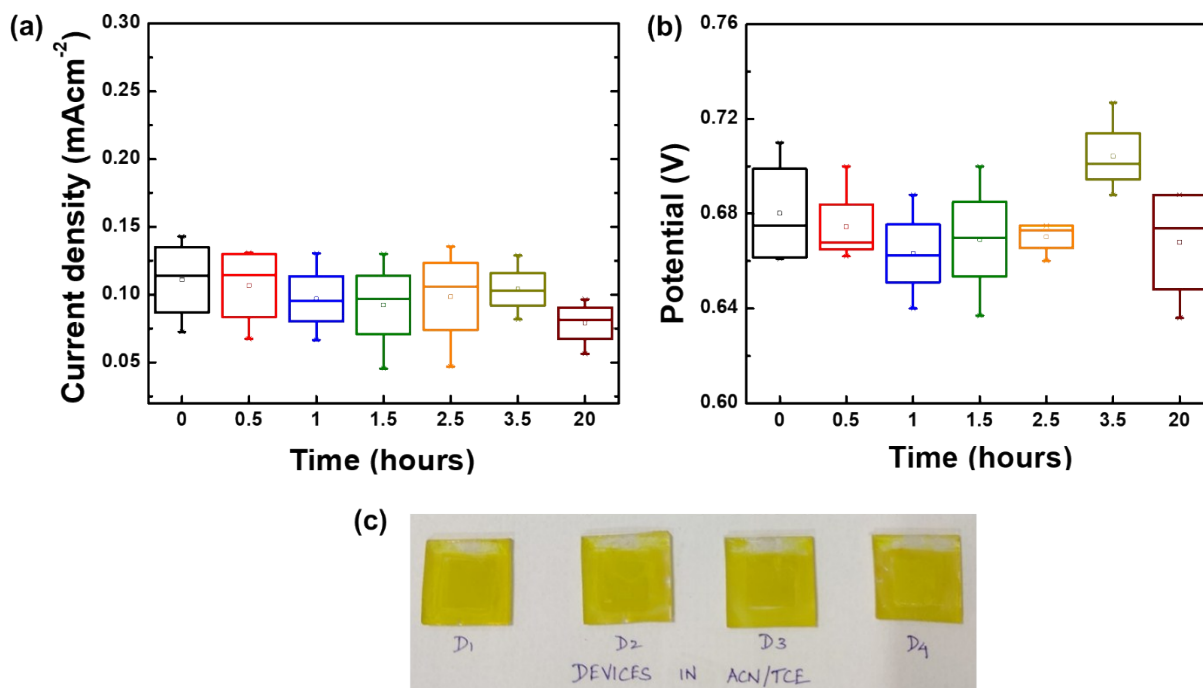


**Figure S4.** Stability test of  $\text{Cs}_2\text{AgBiBr}_6$  PEC solar cell containing  $\text{Co}^{2+}/\text{Co}^{3+}$  electrolyte in tetrachloroethane and acetonitrile (90/10 v/v) carried out over 20 hours. (a) Variation of short-circuit current density, (b) variation of open-circuit potential with time, and (c) photoelectrodes after the stability test. D1-D4 indicated different devices made under the same condition.

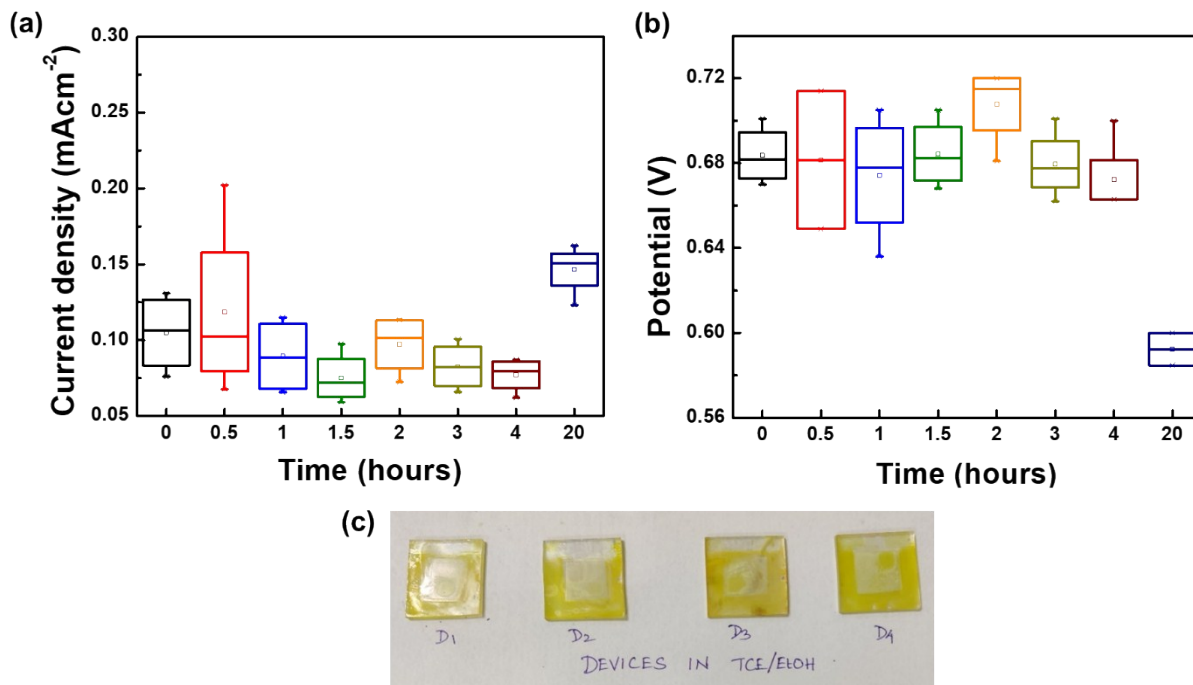


**Figure S5.** Stability test of Cs<sub>2</sub>AgBiBr<sub>6</sub> PEC solar cell containing Co<sup>2+</sup>/Co<sup>3+</sup> electrolyte in tetrachloroethane and ethanol (90/10 v/v) carried out over 20 hours. (a) Variation of short-circuit current density, (b) variation of open-circuit potential with time, and (c) photoelectrodes after the stability test. D1-D4 indicated different devices made under the same condition.

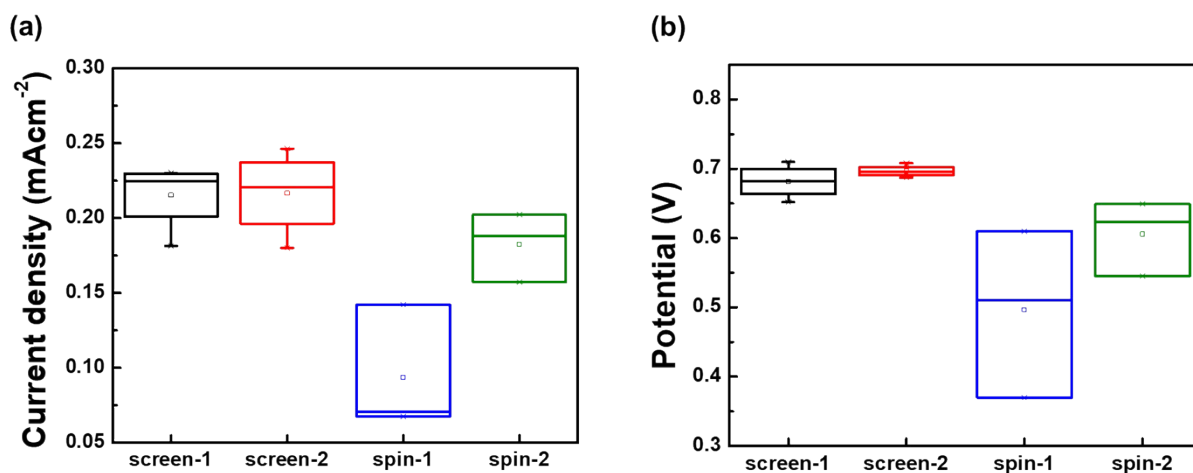


**Figure S6.** Optimisation of the TiO<sub>2</sub> mesoporous underlayer scaffold. (a) Variation of short-circuit current density, and (b) variation of open-circuit potential for different titanium dioxide layers.

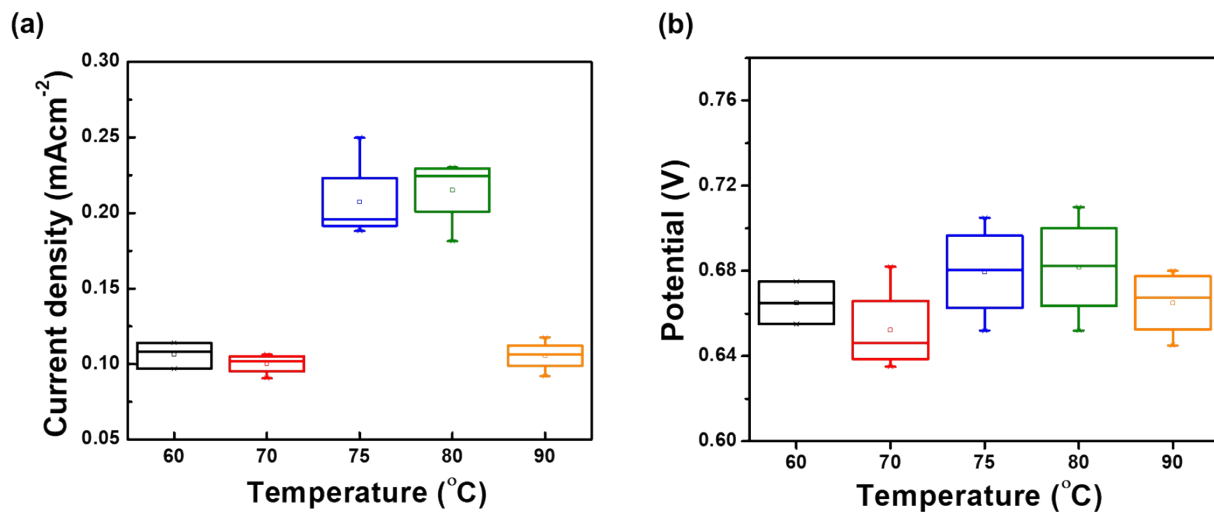


**Figure S7.** Optimisation of the precursor preheating temperature between 60°C and 90°C. (a) Variation of short-circuit current density, and (b) variation of open-circuit potential

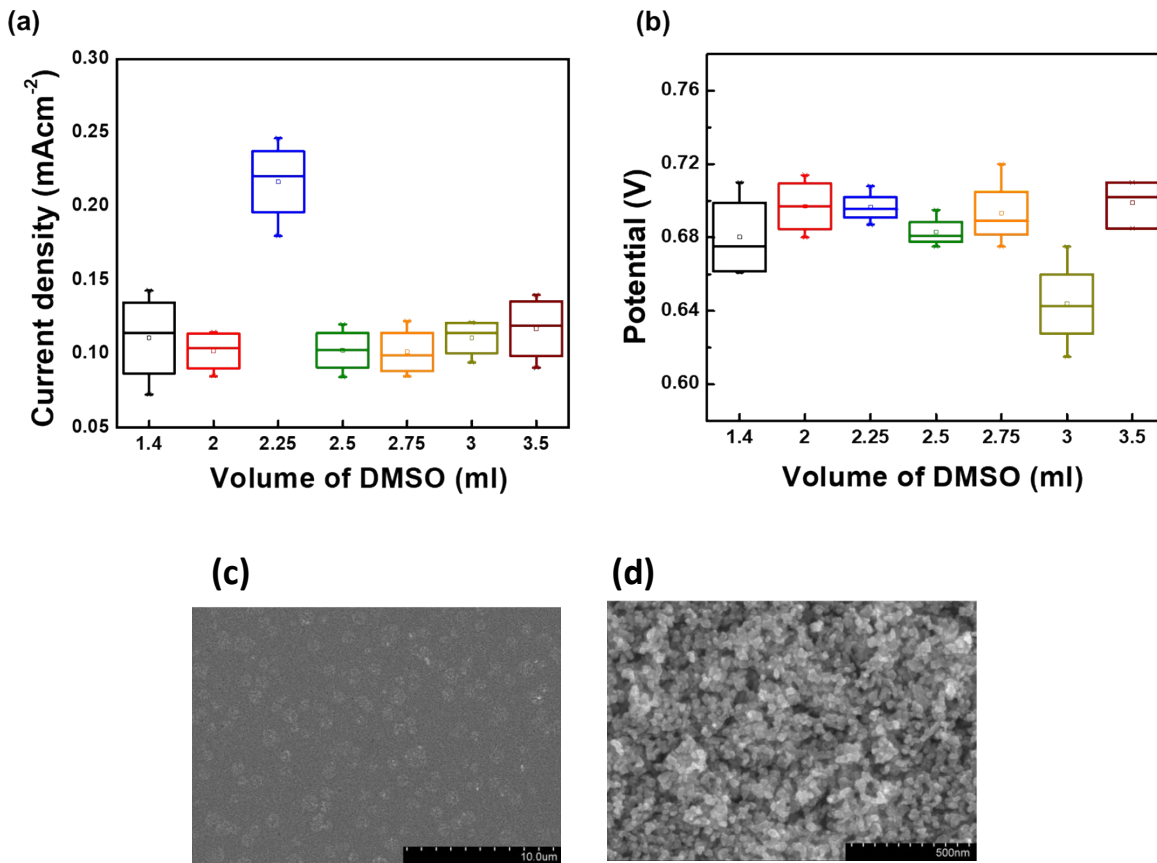


**Figure S8.** Optimisation of the precursor dilution volume. (a) Variation of short-circuit current density, (b) variation of open-circuit potential, and (c,d) micrographs of the annealed film formed by diluting the precursors in 2.25 ml of DMSO.

Mesoporous titanium dioxide substrate is used in this work for the deposition of Cs<sub>2</sub>AgBiBr<sub>6</sub>. The porosity in the film is required for shuttling the redox mediators in and out of the photoanode. From the SEM images, near conformal deposition of perovskite on the substrate shall be observed and also retained the porosity. The uniformity in deposition is expected to ensure proper diffusion of charges in and out of pores, without leading to any mass transport limitation, which is expected with large redox shuttles like cobalt complexes.



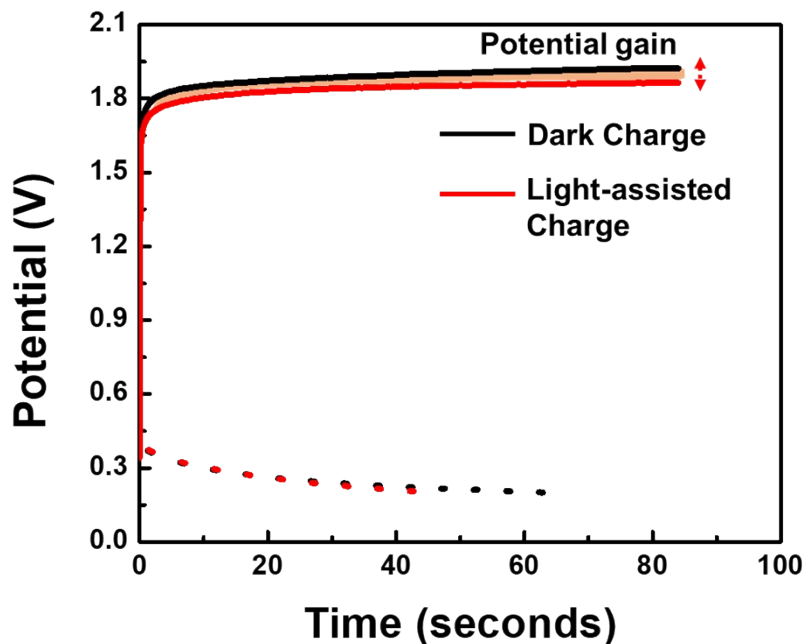


**Figure S11.** Second charge-discharge cycle of PEC energy storage device (photoactive area  $1\text{cm}^2$  and mediator concentration of  $10\text{mM}$ ) under light and dark with a charging current of  $100\mu\text{A}$  and a discharge current of  $5\mu\text{A}$ .

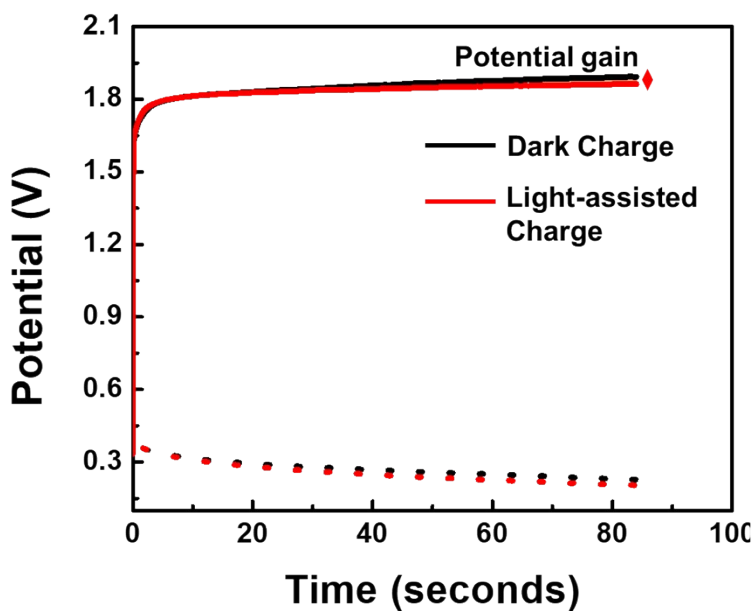


**Figure S12.** Third charge-discharge cycle of PEC energy storage device (photoactive area  $1\text{cm}^2$  and mediator concentration of  $10\text{mM}$ ) under light and dark with a charging current of  $100\mu\text{A}$  and a discharge current of  $5\mu\text{A}$ .

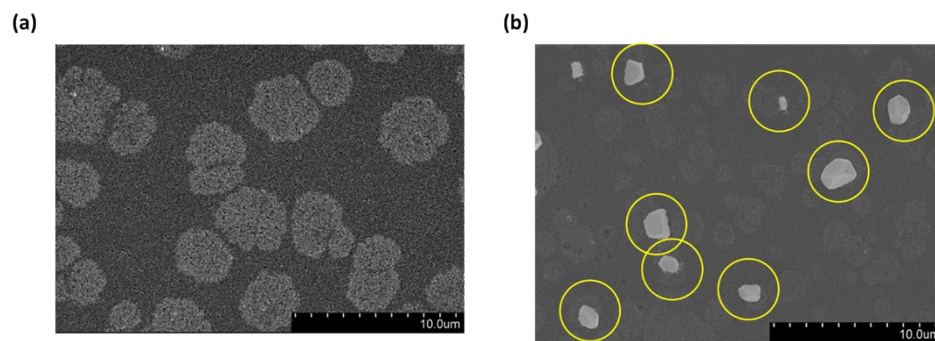


**Figure S13.** Micrographs of the film (formed by diluting the precursors in 1.4ml of DMSO) (a) before use in the energy storage device, and (b) after the 1<sup>st</sup> charge.

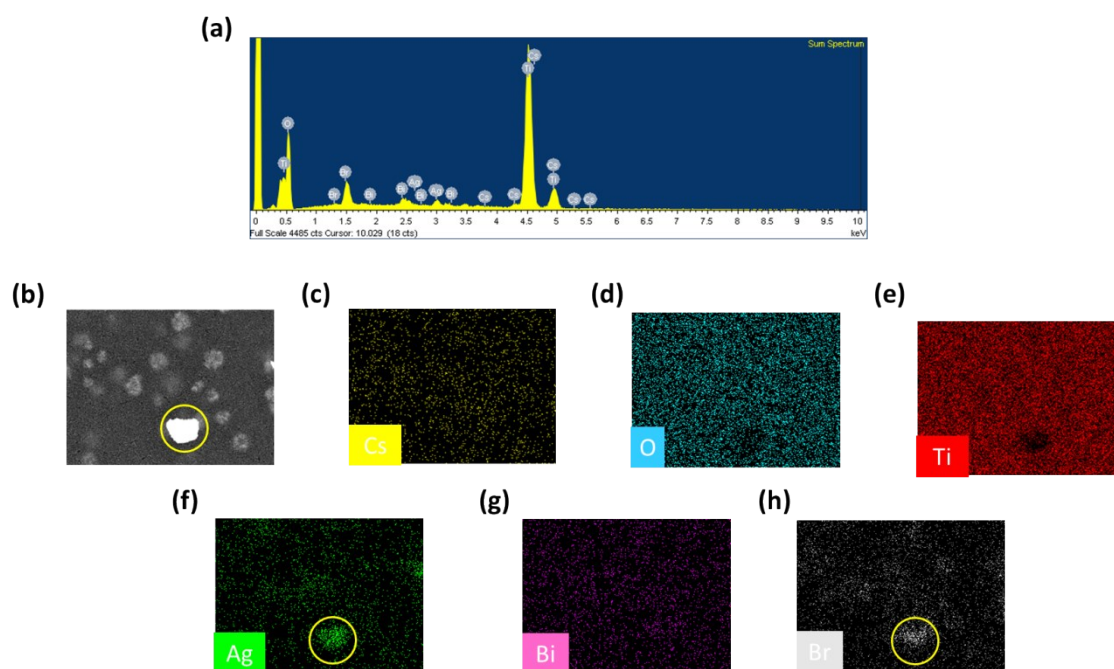


**Figure S14.** EDX spectrum and elemental maps of the film (formed by diluting the precursors in 1.4ml of DMSO) after the first charging cycle. Yellow circles highlight the presence of AgBr. These elemental maps correspond to the SEM given in Figure 13(b)

**Table S1.** Table illustrating the compatibility of the various solvents with the perovskite ( $\text{Cs}_2\text{AgBiBr}_6$ ), solubility of the redox mediator, supporting electrolyte and stability of the membrane.

Solvent	Perovskite	$\text{Co}^{2+}$	$\text{Co}^{3+}$	$\text{MV}_2\text{Cl}_2$	$\text{MV}_2(\text{PF}_6)_2$	TBAPF <sub>6</sub>	DSV membrane
Acetonitrile	unstable	soluble	soluble	insoluble	soluble	soluble	stable
Toluene	stable	soluble	insoluble	insoluble	insoluble	insoluble	stable
Dichloromethane	stable	soluble	insoluble	insoluble	insoluble	soluble	unstable
Chloroform	stable	soluble	insoluble	insoluble	insoluble	soluble	stable
Tetrachloroethane	stable	soluble	insoluble	insoluble	insoluble	soluble	stable

**Table S2.** Comparison of performance and stability of solar assisted rechargeable battery configurations involving a direct liquid junction contact with the photoelectrode.

<sup>a</sup>The photopotential gain is a function of charging current. The charging current differs in different reports.

Positive Electrode	Negative Electrode	Electrolyte	Separator	Number of cycles	Potential gain <sup>a</sup>
$\alpha\text{-Fe}_2\text{O}_3$ <sup>5</sup>	Lithium	Posolyte: 1 M KI, 0.03 M LiI, and 0.08 M I <sub>2</sub> in H <sub>2</sub> O Negolyte: LiTFSI in EC/DMC	Ceramic Membrane (Li <sub>2</sub> O-Al <sub>2</sub> O <sub>3</sub> -TiO <sub>2</sub> -P <sub>2</sub> O <sub>5</sub> )	30 cycles	660mV
TiO <sub>2</sub> -N719-Cu <sub>2</sub> S <sup>6</sup>	Lithium	LiTFSI	-	20 cycles	~350mV

FTO-Z907 <sup>7</sup>	Lithium	Posolyte: 2.00 M LiI, 0.05 M I <sub>2</sub> , and 0.50 M guanidine thiocyanate in saturated chenodeoxycholic acid aqueous solution	-	25 cycles	~600mV
FTO-N719 <sup>8</sup>	Lithium	4.18 mM I <sub>2</sub> , 0.1 M LiI and 1 M LiClO <sub>4</sub> in DMSO.	Glassy fiber, Whatman	25 cycles	~600mV
<b>FTO/ Cs<sub>2</sub>AgBiBr<sub>6</sub> (this work)</b>	<b>Pt/FTO</b>	<b>Posolyte: 10mM Co<sup>2+</sup>/Co<sup>3+</sup>and 10mM TBAPF<sub>6</sub> in ACN</b>  <b>Negolyte: 10mM MV<sup>2+</sup>and 10mM TBAPF<sub>6</sub> in ACN</b>	<b>Selemon DSV</b>	<b>3 cycles</b>	<b>490 mV</b>

The selection of redox shuttles and the solvents for electrolyte is a key factor which hampered the demonstration of solar energy storage in the PEC cell. We have identified cobalt complex and methyl viologen redox couples in tetrachloroethane and acetonitrile solvents, respectively, for electron donor and acceptor. Cascaded device architecture with photocharging and discharging compartments were designed. Using Cs<sub>2</sub>AgBiBr<sub>6</sub> halide double perovskite absorber, a photopotential gain of 490mV was achieved, due to the photogenerated voltage achieved in the absorber. The photopotential gain with the well established dye-sensitizer based PEC cells lie between 350mV and 660mV. In this work with halide perovskites, 490mV gain is achieved, which is on par with the reported values for other dye-sensitized systems. In terms of stability, we have shown three cycles, whereas the prior reports show around 20 to 30 cycles. The reported photoassisted charging devices typically employ iodide/triiodide redox shuttle which has low recombination kinetics unlike cobalt redox mediators. However the former redox system is not compatible with halide perovskites. The self-discharge, electrolyte crossover between compartments and AgBr segregation are found to be detrimental factors affecting device performance. So, further work should involve addressing these issues; specifically, (i) an appropriate membrane that is selective for PF<sub>6</sub><sup>-</sup> anion to eliminate the crossover which in-turn is expected to increase the cycle life/device stability, (ii) fabricating the devices in oxygen free environment to avoid the self-discharge, (iii) passivating the surface of perovskite to reduce

recombination and, (iv) implementing a flow-setup with electrolyte tanks like redox flow batteries.

## REFERENCES

- 1 E. Greul, M. L. Petrus, A. Binek, P. Docampo and T. Bein, *J. Mater. Chem. A*, 2017, **5**, 19972–19981.
- 2 A. Manjula and M. Nagarajan, *Arkivoc*, 2001, **2001**, 165–183.
- 3 S. M. Feldt, E. A. Gibson, E. Gabrielsson, L. Sun, G. Boschloo and A. Hagfeldt, *J. Am. Chem. Soc.*, 2010, **132**, 16714–16724.
- 4 C. Kong, L. Qin, J. Liu, X. Zhong, L. Zhu and Y. T. Long, *Anal. Methods*, 2010, **2**, 1056–1062.
- 5 G. Nikiforidis, K. Tajima and H. R. Byon, *ACS Energy Lett.*, 2016, **1**, 806–813.
- 6 C. Xu, X. Zhang, L. Duan, X. Zhang, X. Li and W. Lü, *Nanoscale*, 2020, **12**, 530–537.
- 7 M. Yu, W. D. McCulloch, D. R. Beauchamp, Z. Huang, X. Ren and Y. Wu, *J. Am. Chem. Soc.*, 2015, **137**, 8332–8335.
- 8 M. Yu, X. Ren, L. Ma and Y. Wu, *Nat. Commun.*, 2014, **5**, 1–6.